Quasi-static cyclic tests of Emulative Precast Segmental Bridge Piers (E-PSBP)

M. Mashal, S. White, & A. Palermo

Department of Civil and Natural Resources Engineering, University of Canterbury, Christchurch.

2013 NZSEE Conference

ABSTRACT: The use of precast segmental columns is a particular feature of Accelerated Bridge Construction (ABC) of bridges. The technology of precasting bridge substructure systems offers many advantages in the construction process. In particular for multiple spanned structures, it includes reduced construction time, minimal traffic disruptions, reduced life cycle costs, and improved construction quality and safety. There are a number of examples internationally of precast substructure systems, mainly in areas of low seismicity.

Precast Segmental Bridge Piers (PSBP) comprise of precast concrete elements, connected using a number of options including grouted duct connections, mechanical couplers, post-tensioned tendons, and member socket connections.

The majority of low to medium span bridges around New Zealand have cast in place (CIP) bridge piers. PSBP can be designed to emulate the behavior of conventional CIP substructures (Emulative Segmental Bridge Piers or E-PSBP) through formation of plastic hinges in the piers under earthquake loading. This results in a system with good lateral load capacity giving potential for use in regions of high seismicity.

This paper presents current experimental research into the uni-directional seismic performance of two half-scaled E-PSBP specimens designed for a prototype bridge with a 12 meter span length representing a typical New Zealand highway bridge. The first specimen has a square section with grouted duct connection. The second specimen has a circular section with member socket connections. Both specimens performed satisfactorily in a similar manner that would be expected from a monolithic connection. The experimental program underway at the University of Canterbury (UC) is a part of an extensive project titled Advanced Bridge Construction and Design (ABCD) funded by the Natural Hazard Research Platform.

1 INTRODUCTION

CIP substructure systems for bridges have been the most common construction practice in New Zealand, regardless of bridge dimensions (span lengths, pier heights). CIP gives the advantage of saving cost for the formwork if standard column shapes (circular or square) are used. Nowadays bridges with spans of 12m to 30m incorporate precast superstructure system that can be either continuous or simply supported. The construction time of CIP substructures can be lengthy with severe disruption to traffic especially in populated areas. Following the Canterbury earthquakes, the repair and replacement work of damaged bridges in Christchurch is a clear example of such delays and disruptions. Other challenges with CIP construction include but are not limited to fast project delivery, better material quality control, more accuracy in dimensions of the substructure elements, higher level of safety, and minimized environmental impacts. General background has been summarized in (Palermo and Mashal 2012).

Precast Segmental Bridge Piers (PSBP) provides a solution to the above challenges. PSBP offer many advantages in construction of bridge substructure systems and have already been in use in low seismicity areas. However, the use of PSBP in high seismic regions has been limited due uncertainty in the seismic performance of such systems. Over the past several years, there has been increasing

attention given to PSBP (Ou et al., 2012). A notable example is research into standardized precast substructure systems by Billington et al. (1999). There has also been significant interest into ABC by US Departments of Transportation including Washington (Khaleghi, 2010), Texas (Ralls et al., 2004), Utah (Utah DOT, 2008) (Burkett et al., 2004) and The Federal Highway Administration (U.S. FHWA, 2011).

Emulative PSBP aims to emulate the hysteretic behavior of a conventional CIP pier with one using precast segmental piers. The emulative behavior allows direct use of the current seismic design codes. This paper proposes E-PSBP construction as an alternative to CIP substructure system for bridges with small to medium span length (12 – 30m) in New Zealand. E-PSP systems are designed and detailed to achieve plastic hinges similar to those of CIP piers allowing conventional design procedures to be adopted. This paper presents the findings of testing that aims to verify that the columns do in fact perform in a similar manner.

2 DEVELOPMENT OF SPECIMENS

2.1 Prototype selection and design considerations

The prototype bridge dimensions are based on a typical bridge with small span length (12m) in New Zealand as shown in Figure 1 (right). The bridge has single pier supports with a gravity load of 1810kN on each pier. The deck system for the prototype consists of Dual Hollow Core (DHC) sections described in NZTA Research Report 364 (2008). The bridge is located in Christchurch which is a high seismic region with the hazard parameters shown in Figure 1 as per NZS 1170.5 (2004). According to NZTA Bridge Manual (2003) for earthquake resistant design of the prototype shown in Figure 1 (right), the energy dissipation system relies on a ductile or partially ductile structure. In this case the plastic hinges form at design load intensity in the pier above the ground level, refer to Figure 1 (left). The maximum allowable design displacement ductility is 6 for this type structure.

For this research, two specimens have been developed for quasi-static uni-directional testing. The specimens are half the scale of the prototype shown in Figure 1 (right). The specimens include one square and one circular section. An assumed ductility (μ =3) has been used for the seismic design of the specimens. NZS 1170.5 (2004) is used for the seismic loading. The specimens are designed and detailed according to the current edition of NZS 3101 (2006). Piers were designed using Ø=1 to obtain an estimation of actual strength of the section for testing. The section design and method of construction for each pier specimen are discussed in subsequent sections.

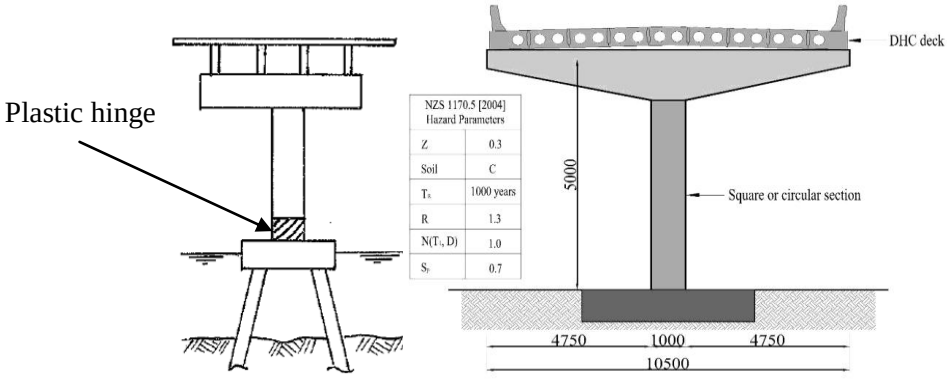

Figure 1 Prototype bridge support; (left) plastic hinge location; (right) front elevation

3 SEISMIC DETAILING AND PROPOSED METHOD OF CONSTRUCTION

3.1 Material properties

Table 1 provides a summary of material properties for the specimens.

Table 1. Summary material properties

	SQ1 (Square)				CR1 (Circular)			
	Pier		Footing		Pier		Footing	
Strength (MPa)	**Specified**	**Actual**	**Specified**	**Actual**	**Specified**	**Actual**	**Specified**	**Actual**
Longitudinal Steel f_y	500	516	500	516	500	516	500	516
Transverse Steel f_s^*	500	556	500	516	500	556	500	516
Concrete f'_c	40	60	35	59	40	54	40	43
Grout $f'_m{}^*$	60	64	60	64	50	55	50	58

3.2 **Specimen No 1 (SQ1)**

The first specimen, SQ1, has a square section (Figure 2) supporting a gravity load of 450kN. Grouted Duct Connection (GDC) is used for segment to segment and the first segment to spread footing connections. In this type of connection, the reinforcing bars from one precast member are inserted into ducts which are cast into the second element. Grout is pumped into the ducts after assembling and aligning the segments on top of each other.

The GDC has already been used in non-seismic and seismic regions. There is a significant amount of research done on this type of connections (NCHRP Report 698, 2011). It has been a common construction technique for precast concrete columns in New Zealand. However, most of these applications have been limited by using GDC in capacity protected or lower demand zones in structures. The use of GDC in plastic hinging zone in a high seismicity region has been limited. This study covers application of GDC in expected plastic hinge zone. Experimental testing is carried out to confirm if commonly designed CIP plastic hinging can be obtained by using GDC. It can also be used for pile to pile cap, spread footing or pile cap to column, column to cap beam and for splices between column segments or cap beam segments. The seismic performance, durability, and inspectability of GDC are similar to CIP. The construction risk can be less favorable compared to CIP because of possible difficulties with alignment of grouting ducts.

For the construction of SQ1, a shear key was placed between each joint. This shear key was designed similar to a corbel to resist the exerted shear forces between segment to segment and segment to footing joints in the column. The shear key was later grouted inside the socket to emulate a monolithic type of connection, refer to Figure 2. There was a maximum 20mm gap between the segments for the mortar bed. The grout was pumped through the drilled holes inside the ducts. For both specimens, it was assured that that grout should have higher compressive strength than the surrounding concrete as presented in Table 1. Figure 4 shows the components for SQ1 and the assembled specimen.

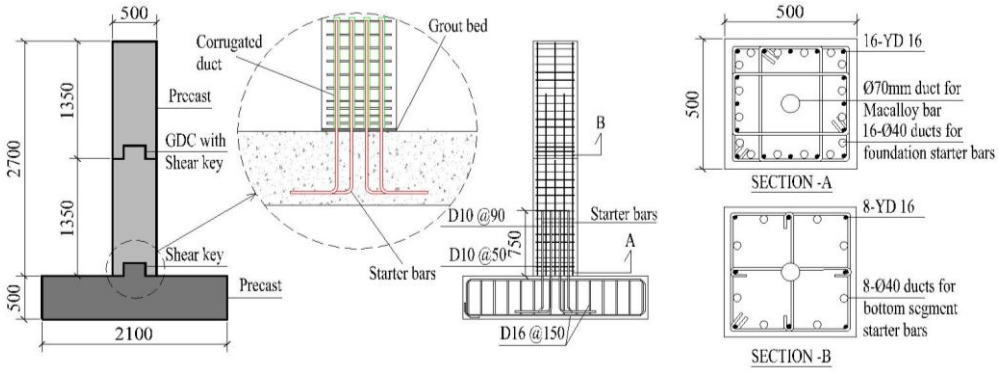

Figure 2 Section details for SQ1 with GDC

3.3 **Specimen No 2 (CR1)**

The second specimen, CR1, has a circular section (Figure 3) supporting the same gravity load as SQ1. The segments are joined using GDC with a shear key as in SQ1. The first segment to spread footing connection is a Member Socket Connection (MSC). The MSC is formed by embedding a precast element inside another element which can be either precast or CIP. If both elements are precast, then the connection is secured using a grout or concrete closure pour in the preformed socket. The other solution is to have the second element cast around the first one. The MSC has been used in buildings with a few examples in bridges, (NCHRP, 2011). This type of connection can be used for footing to column, column to cap beam, and pile to pile cap locations. For the construction of CR1, the segments were joined similar to SQ1 (GDC). The first segment to precast footing joint was secured using grout. Before grouting, the surfaces around the end of the column and the hole in footing were roughened for a better bond between the grout and concrete. The roughening of the surface can be simply done by applying a roughening liquid agent around the formwork before pouring of concrete at the fabrication yard. Figure 5 shows the components for CR1 and the assembled specimen.

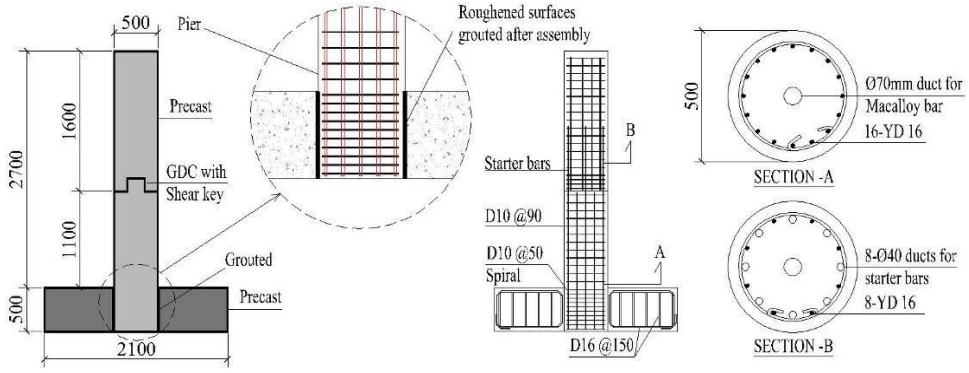

Figure 3 Section details for CR1 with MSC

Figure 4 Assembled specimen SQ1 (left); segmental columns (middle); spread footing (right)

Figure 5 Assembled specimen CR1 (left); segmental columns (middle); spread footing (right)

4 EXPERIMENTAL TESTING

4.1 Test setup and loading protocol

The columns were subjected to uni-directional pseudo-static testing. The specimens were tested using the ACI T1-01 (2001) loading protocol. The displacement history used for testing is shown in Figure 6 (right). Lateral load was applied to the columns at a height of 3m above the floor using a 400KN ram attached to a reaction frame. The axial load was simulated using an un-bonded 40mm Macalloy bar located at the center of the columns (Figure 6, left) with the load kept within tolerance of < 5% (20kN) throughout testing by regulating axial jack pressure.

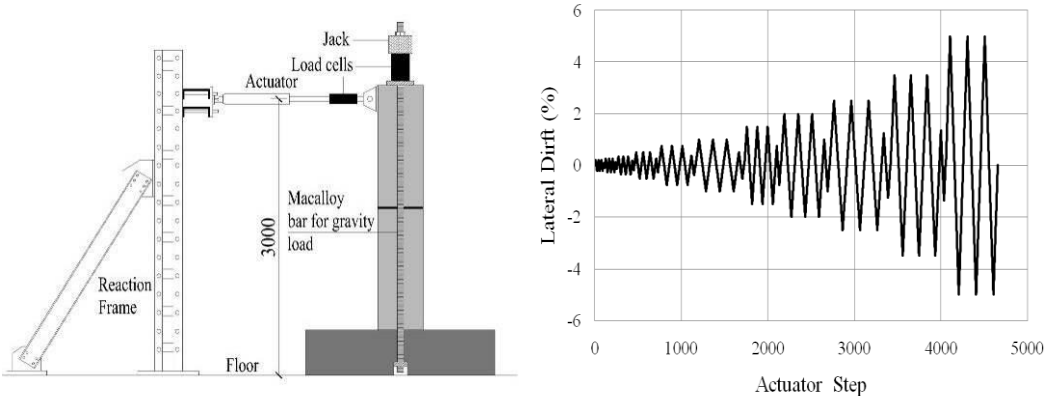

Figure 6 Uni-directional testing setup (left); displacement history (right)

4.2 Experimental performance

4.2.1 *Specimen 1 (SQ1)*

Minor flexural cracking of the grouted joint at the base of the columns initiated at a drift of 0.35%. Further cracks appeared throughout the segments during the 0.5% drift cycle and increased in density throughout larger cycles with no significant increase in width. The width of the majority of cracks remained less than 0.4mm during testing with most of the deformation in the column constrained to the grouted regions of the column, in particular the grouting bed between column and spread footing where the grout was deteriorated to an increased width of 7mm at 3% drift.

Spalling of concrete occurred during the 3% drift cycle. The extent of spalling increased during the 4% drift cycle reaching a height of approximately 200mm above the top face of the footing. Bar rupture occurred at a drift of 5.0%, see Figure 9 (left). By the end of the test, spalling occurred to a height of approximately 250mm.

From the load-displacement plot (Figure 7, left) showing ram displacement against ram load, it can be seen that the column yielded at a displacement of 19mm corresponding to a drift of 0.75%. This gives a displacement ductility of 4 when considering spalling as the ultimate limit state (ULS) from NZS 3101 (2006). The ductility at failure point was greater than 6 in this case. Large residual displacements were observed for drift cycles larger than the yield drift with the residual displacement equaling greater than half the peak displacement for the 4% and 5% drift cycles.

The column achieved a peak base shear of 207kN corresponding to a moment capacity of 518kNm. This is larger than the design base shear of 167kN. Figure 8 shows the moment curvature behavior of the column along with the theoretical moment-curvature curve using actual material strengths.

Upon inspection following disassembly, it was found that grout had flowed into the central duct causing the Macalloy bar to become bonded across the interface between footing and column. As the column was displaced, there was no load increase in the Macalloy bar indicating that the bar was fully bonded across the interface where most of the deformation was observed. This meant that the axial load provided by the Macalloy bar was only acting in the column above the interface between footing

and column with no axial load being transferred to the footing. The Macalloy bar was acting as a bonded reinforcement bar causing the observed curvature curve to lie below the theoretical curve for low levels of drift and above the theoretical curve for high levels of drift as the bar picked up load. Limitations on the test results are stated in conclusions.

4.2.2 *Specimen 2 (CR1)*

Cracks in the second specimen initiated during the 0.25% drift cycle. Further cracking occurred at higher levels of drift with a similar distribution of cracks as the first segment but larger crack widths towards the base of the column indicating more distribution of inelastic deformation in the column.

Minor spalling of concrete initiated during the 3% drift cycle with the extent of spalling increasing during larger drift cycles. During the 6.0% drift cycle, spalling had extended to approximately 500mm from the top face of the footing, see Figure 9 (right).

During the 6.0% drift cycle, the column could be pushed to 6.0% drift but only pulled to 5.2% drift due to limitations in the stroke distance of the ram. The column completed the 6.0% drift cycle with no bar rupture. Bar rupture occurred in the following drift cycle as the column reached 6.0% drift. Since the column did not experience bar rupture in the first instance of reaching a drift of 6.0%, it is apparent that low cycle fatigue contributed to bar failure.

The load-displacement plot (Figure 7, right) shows that the column yielded at a drift of 1% corresponding to a displacement ductility of 3 when considering spalling as the ultimate limit state. The ductility at failure point was equal to 6. The residual displacements observed in the second column were slightly smaller than those of the first column but still significant. The column achieved a peak base shear of 156kN corresponding to a moment capacity of 390kNm which is within 5% of the design base shear of 162kN.

A good correlation between the theoretical and experimental moment-curvature plots was observed in the second column indicating the Macalloy bar performed as desired in simulating the axial load.

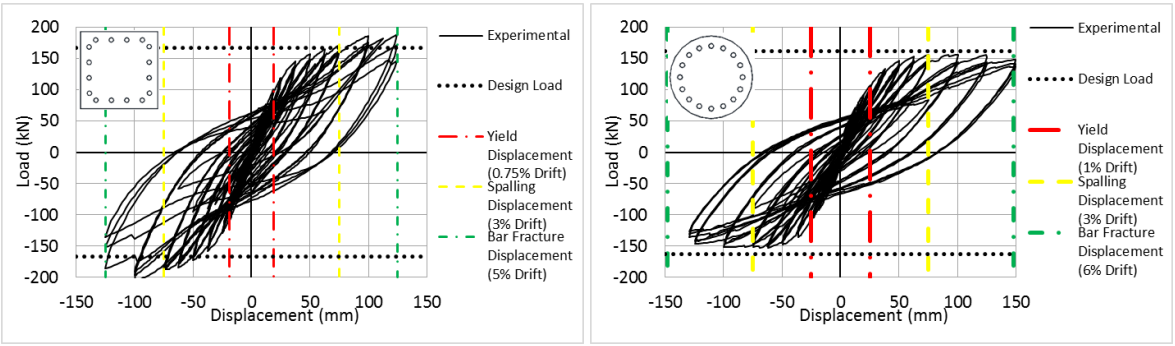

Figure 7 Force-displacement plot; SQ1 (left); CR1 (right)

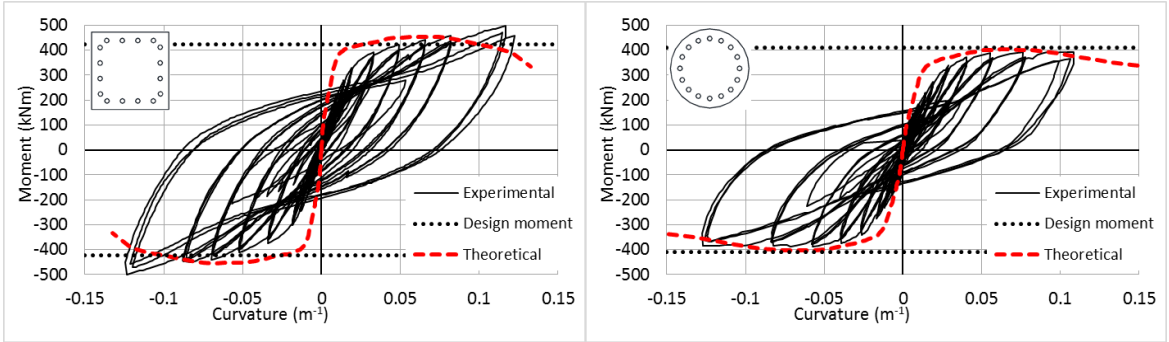

Figure 8 Moment-curvature plot; SQ1 (left); CR1 (right)

Figure 9 Plastic hinging of the base; SQ1 at 5% drift (left); CR1 at 6% drift (right)

5 DISCUSSION AND SUMMARY OF THE PERFORMANCE

Riva (2006) describes the cyclic performance of GDC based on the testing of the column to foundation connection. The results from Riva (2006) show similar findings as the ones presented in this research. The grouting bedding layer deteriorated with cyclic loading; the consequence is that compression forces have to be resisted by the starter bars confined in the grouted ducts. This resulted in stiffness degradation and a pinched hysteresis loop with a slight reduction in energy dissipation capacity when compared with a CIP connection.

From the seismic performance aspect, the use of fibers for reinforcing the bedding layer can be an option for controlling degradation. However; this yet has to be confirmed (NCHRP, 2011). The cold joint at the base of the column and damage in the grout bedding layer leads to concentration of inelastic deformation at the base of the column, which causes a plastic hinge with shorter length compare to CIP. This shorter plastic hinge length caused a higher level of strain in the longitudinal bars at the column-footing interface for a given level of lateral column displacement leading to rupture of the bars at a lower level of drift. There is a bi-directional testing scheduled to be undertaken on an identical column as SQ1 with the same GDC at UC. The base of column will be armored to prevent buckling of the bar, as well as leaving a deboned length in starter bars for better strain distribution.

During testing of CR1 which incorporated MSC, the foundation remained intact. The majority of inelastic deformation was observed at the base of the column with more distributed cracking than observed in the GDC connection. Similar results can be found in Riva (2006) where the MSC had exhibited more distributed cracking of the column than both the GDC and CIP. By providing sufficient confinement to prevent from buckling of the vertical bars, the failure mechanism was initiated by rupture of the longitudinal bars in tension after carrying several cycles of loading at 6% drift.

During cyclic loading of the MSC, there was no observed rotation or cracking of the gout at the bottom of footing. This implies that the connection had sufficient strength to force failure of the pier into the designated plastic hinge region of the column, avoiding inelastic deformation of the column-footing connection. In order to find the residual gravity load carrying capacity of the column, a punching shear test was undertaken on the column-footing socket. The test was done by cutting off the column at the column-footing interface. Then, placing a high capacity hydraulic jack underneath the footing within the socket area and pushing upwards. The footing would be tied to the floor using high strength anchor rods. The socket was loaded to a 1500kN force (3 times greater than its gravity design load); there was no movement in the socket or breaking of the grouting recorded. The grout initially had a minimum gravity load carrying strength of more than 6 times of the gravity load design after 7 days of pouring. The residual capacity after lateral loading was proven to be at least 3 times greater than the gravity design load. The roughening of the surface around the base of precast column and the socket in the foundation was very effective in providing a good column to foundation bond for transfer of gravity loads.

5.1 **Conclusions**

The experimental testing showed promising results for both the GDC and MSC with both achieving good strength and ductility. Both showed slightly pinched hysteresis loops which reduce the energy dissipation capabilities of the systems when compared with CIP piers however this is unlikely to have a significant effect on seismic performance. Both connections provide the potential for significant time savings through avoiding the need for assembly of formwork and pouring of concrete on site. The use of precast elements offers higher levels of quality control, leading to more accurate construction of substructure elements and higher construction quality. Limitations of test results for GDC caused by grouted Macalloy bar can be explained as it did not compromise the whole behavior of the specimen. The grouted Macalloy bar could have compromised only the capacity but not ductility of the column. Testing is currently underway at the University of Canterbury to further explore the behavior of the GDC and MSC for the identical column specimens in this paper under bi-directional loading and later to investigate low damage connection options.

5.2 **Acknowledgments**

The authors would like to express their gratitude to the Ministry of Science and Innovation (MSI) – Natural Hazard Research Platform for supporting this research as part of the project ABCD.

5.3 **References**

ACI T1.1-01 2001. Acceptance Criteria for Moment Frames Based on Structural Testing, *ACI Innovation Task Group*, Farmington Hills, Michigan, United States.

Billington, S. L., Barnes, R. W., & Breen, J. E. (1999). A Precast Segmental Substructure System for Standard Bridges. J. Precast/Prestressed Concrete Inst., 44(4), 56-73.

Bridge Manual 2nd Edition 2003. *New Zealand Transportation Agency (NZTA),* Wellington.

Billington, S. L., Barnes, R. W., & Breen, J. E. (1999). A Precast Segmental Substructure System for Standard Bridges. J. Precast/Prestressed Concrete Inst., 44(4), 56-73.

Burkett, W. R., Nash, P. T., Bai, Y., Hays, C., & Jones, C. (2004). Rapid Bridge Replacement Techniques Research Report.

Khaleghi, B. (2010). Washington State Department of Transportation Plan for Accelerated Bridge Construction. Transportation Research Record: Journal of the Transportation Research Board, 2200(-1), 3-11. doi: 10.3141/2200-01

NCHRP Report 698 2011. Application of Accelerated Bridge Construction Connections in Moderate-to-High Seismic Regions, *Transportation Research Board,* Washington D.C., United States.

NZS 3101 2006. Part 1 The Design of Concrete Structures, *New Zealand Standards,*Wellington.

NZS 1170.5 2004. Structural Design Actions, Part 5: Earthquake Actions, *New Zealand Standards,* Wellington

NZTA Research Report 364 2008. Standard Precast Concrete Bridge Beams, *New Zealand Transportation Agency (NZTA),* Wellington.

Ou, Tsai, Oktavianus & Chang 2012. Cyclic Testing of a Tall Precast Segmental Concrete Bridge Column with a Cast-In-Place Plastic Hinge Region, *6th International Conference on Bridge Maintenance, Safety, and Management (IABMAS*), July 8-12 2012 , Stresa, Italy.

Palermo, A. & Mashal, M. 2012. Accelerated Bridge Construction and Seismic Damage Resistant Technology: A New Zealand Challenge, *NZSEE Bulletin*, Vol. 45, No. 3, Wellington

Ralls, M. L., Hyzak, M. D., Medlock, R. D., & Wolf, L. M. (2004). Prefabricated Bridges - Current U.S. Practice and Issues FHWA/AASHTO Second National Prefabricated Bridge Elements & Systems Workshop. New Brunswick, New Jersey.

Riva, P. 2006. Seismic Behaviour of Precast column-to-Foundation grouted Sleeve Connections. *Proceeding of International Conference on Advances in Engineering Structures, Mechanics & construction*, Waterloo, Ontario, Canada, pp. 121-128.

Utah DOT. (2008). Utah Department of Transportation Accelerated Bridge Construction Standards Workshop.

U.S. FHWA. (2011). Accelerated Bridge Construction Manual